

1 **Supported ionic liquid membrane based on [bmim][PF₆] can be a**
2 **promising separator to replace Nafion in microbial fuel cells and improve**
3 **energy recovery: A comparative process evaluation**

4
5 László Koók¹, Barbara Kaufer¹, Péter Bakonyi^{1,*}, Tamás Rózsenberszki¹, Isaac
6 Rivera², Germán Buitrón³, Katalin Bélafi-Bakó¹, Nándor Nemestóthy¹

7
8 ¹Research Institute on Bioengineering, Membrane Technology and Energetics,
9 University of Pannonia, Egyetem ut 10, 8200 Veszprém, Hungary

10
11 ²Institute of Environmental and Sustainable Chemistry, TU-Braunschweig,
12 Hagenring 30, 38106 Braunschweig, Germany

13
14 ³Laboratory for Research on Advanced Processes for Water Treatment,
15 Instituto de Ingeniería, Unidad Académica Juriquilla, Universidad Nacional
16 Autónoma de México, Blvd. Juriquilla 3001, Querétaro 76230, Mexico

17
18
19
20
21 *Corresponding Author: Péter Bakonyi

22 Tel: +36 88 624385

23 E-mail: bakonyip@almos.uni-pannon.hu

25 **Abstract**

26

27 In this study, mixed culture bioelectrochemical systems were operated
28 with various membrane separators: one prepared with 1-Butyl-3-
29 methylimidazolium hexafluorophosphate ([bmim][PF₆]) ionic liquid and another
30 one called Nafion, used as reference for comparative evaluation. In the course
31 of experiments, the primary objective was to reveal the influence of
32 membranes-type on microbial fuel cell (MFC) behavior by applying a range of
33 characterization methods. These included cell polarization measurements,
34 monitoring of dehydrogenase enzyme activity and cyclic voltammetry for the
35 analysis of anode biofilm properties and related electron transfer mechanism.
36 Additionally, MFC performances for both membranes were assessed based on
37 Coulombic efficiency as well as substrate (acetate) concentration dependency
38 of energy yields. As a result, it was demonstrated that the ionic liquid-
39 containing membrane could be suitable to compete with Nafion and appears
40 as a candidate to be further investigated for microbial electrochemical
41 applications.

42

43 **Keywords:** microbial fuel cell; membrane; separator; ionic liquid; cyclic
44 voltammetry; dehydrogenase enzyme activity

45

46 **Notation list**

47

48 MFC: microbial fuel cell

49 PEM: proton selective/exchange membrane

50 SILM: supported ionic liquid membrane

51 PEM-MFC: MFC equipped with Nafion 115 PEM

52 [bmim][PF₆]: 1-butyl-3-methylimidazolium hexafluorophosphate ionic liquid

53 ILM-MFC: MFC equipped with SILM (containing [bmim][PF₆])

54 IL: ionic liquid

55 PVDF: polyvinylidene difluoride

56 DA: dehydrogenase enzyme activity [$\mu\text{g mL}^{-1}$ toluene]

57 CV: cyclic voltammetry

58 R_e : external resistor in the MFC electric circuit [Ω]

59 R_i : total internal resistance of MFC [Ω]

60 V : electric voltage [mV]

61 I : electric current [mA]

62 P : electric power [mW]

63 I_d : current density normalized to apparent anode surface area [mA m^{-2}]

64 P_d : power density normalized to apparent anode surface area [mW m^{-2}]

65 Y_s : specific energy yield (the electric energy recovered based on the COD added and apparent anode surface area [$\text{kJ g}_{\text{COD,in}} \text{m}^{-2}$])

67 CE: Coulombic efficiency [%]

68 TTC: 2,3,5-triphenyltetrazolium chloride

69 TF: triphenyl formazan

70 CDP: cell design point of MFC

71 OCV: open circuit voltage [mV]

72 E_a : anode electrode potential [mV]

73 E_c : cathode electrode potential [mV]

74 **1. Introduction**

75

76 Among microbial electrochemical systems, MFC technology is currently
77 one of the most rapidly developing one, having the ability to transform the
78 chemical energy (stored in various substrates) into the form of electricity by
79 exploiting the metabolism of so-called exoelectrogenic microorganisms [1]. As
80 it turned out from the research progress of the past years, not only simple
81 compounds (including sugars, alcohols, volatile fatty acids, etc., used mostly in
82 fundamental studies [2]), but also different complex, environmentally-
83 threatening waste streams can be seen as suitable as feedstocks to operate
84 the bioelectrochemical systems [3-8]. thus, MFCs show a good opportunity for
85 the simultaneous management of pollutants and production of electrical
86 energy [9].

87 So far, the widespread application of these biologically-assisted setups
88 has not been typically realized at an industrial level, however, some successful
89 implementations were communicated at real, scaled-up wastewater treatment
90 plants [10, 11]. The reason behind this, as a matter of fact, can be associated
91 with the notable number of existing challenges to be resolved so as to achieve
92 cost-effective operation and decent performance [9, 12]. Some of the hurdles
93 to overcome, besides microbiological aspects, are related to the MFC
94 architecture [13]. Basically, from this point of view, MFCs are classified as
95 single- and two-compartment devices, depending on the actual cell
96 configuration and in particular how the electrodes (anode and cathode, serving
97 as terminal electron acceptors and donors, respectively) are separated from
98 each other [14].

99 In case of dual-chambered constructions, the physical separators,
100 commonly membranes play a remarkable role (i.e. to maintain proton transfer
101 from anode to cathode) and should therefore reflect traits such as (i) chemical
102 stability, (ii) high ionic conductivity (or in other words, low membrane
103 resistance) [15], (iii) appropriate selectivity for protons [16] and low
104 permeability for oxygen (to defend the anaerobic conditions in the anode side)

105 [17]. In addition, the occurrence of pH splitting (the acidification of the anolyte
106 and alkalination of catholyte due to the transport of cations other than protons)
107 [18, 19], substrate cross-over and biofouling can also have significantly
108 negative effect on the current generation capability and overall energy
109 efficiency of MFCs. Hence, the development of membranes that fulfill these
110 requirements and manage to counteract such technological issues are of
111 interest.

112 As of now, PEMs are applied in most laboratory-scale MFC systems,
113 first and foremost made of Nafion [20]. However, in this case, insufficient
114 resistance to oxygen mass transfer and susceptibility of its sulfonate functional
115 groups to be occupied by cations (e.g. Na⁺ and K⁺ instead of protons) can lead
116 to remarkable decrease in MFC performance [21-23]. Recently, promising
117 advancements have been observed in the literature studies employing
118 alternative materials [24-31]. Among them, lately, membrane separators
119 prepared with ILs have gained attention [32-34]. Previously, the potential of
120 using certain SILM instead of Nafion was presented [33]. In a follow-up work
121 [34], the comparative evaluation of such IL-based membrane separators was
122 carried out, yielding useful feedback related to their oxygen and substrate
123 (acetate) mass transfer properties. As a continuation of this research line (to
124 deepen and further improve the knowledge), MFCs assembled with
125 membranes containing [bmim][PF₆] ionic liquid were tested in the present
126 work. The bioprocess was assessed via:

- 127
- 128 - monitoring biological adaptation by dehydrogenase enzyme activity
 - 129 - running cyclic voltammetry (CV) to characterize the mechanism electron
130 transfer
 - 131 - conducting cell polarization to determine total internal resistances,
 - 132 - performing electrochemical impedance spectroscopy (EIS) to evaluate the
133 contribution of (i) charge transfer, (ii) electrolyte (membrane+solution) and
134 implicitly the (iii) diffusion resistances.

135

136 It is believed that the outcomes delivered by this comprehensive
137 (microbiological + electrochemical) approach can assist the better
138 understanding of MFC behaviors (as a function of actual membrane type and
139 characteristics) and in such a way, enrich the relevant literature with
140 important/novel data.

141

142 **2. Materials and Methods**

143

144 **2.1. Supported ionic liquid membrane (SILM) preparation**

145

146 The SILMs were fabricated by immobilizing [bmim][PF₆] ionic liquid
147 (IoLiTec, Germany) in the pores of hydrophobic Durapore PVDF microfiltration
148 supporting membrane (Sigma-Aldrich, USA). The diameters of the PVDF
149 membrane (116 μm mean thickness) and its micropores were 8 cm and 0.22
150 μm, respectively. 3 mL of [bmim][PF₆] was used for membrane preparation
151 and before use, the membrane surface was gently cleaned to remove the
152 excess ionic liquid as much as possible. Until use, the SILM was stored in
153 sealed Petri-dish at room temperature (Some more information about the
154 procedure can be found elsewhere in our previous papers i.e. [33]). As a
155 result, the SILMs contained in average 20.5 mg cm⁻² ionic liquid on basis of
156 (support) membrane surface area. This value is in the same order of
157 magnitude reported in our previous work [33] and also comparable to the
158 those documented by [Hernández-Fernández et al. \[32\]](#) using various IL-based
159 membrane separators in microbial fuel cells. The thickness of the prepared
160 SILMs in contact with electrolytes (swollen-state) was 125 μm in average.

161

162 **2.2. MFC setup**

163

164 The two-chamber, batch MFCs used in this study were made of
165 plexiglass and operated with a working volumes of 160 mL (both anode and
166 cathode sides) (**Fig. 1**). The anode electrode with 26 cm² of apparent surface

167 area was carbon felt (Zoltek PX35, Zoltek Corp., USA), while in the aerated
168 cathode chamber, carbon cloth (0.3 mg Pt cm⁻², FuelCellsEtc, USA) as
169 cathode was used with apparent surface area of 8 cm². Both electrodes were
170 connected to an external circuit through titanium wiring (Sigma-Aldrich, USA).
171 To monitor the potential difference between the anode and cathode
172 electrodes, the circuit comprised of 1 kΩ R_e (**Fig. 2A**), which was changed
173 after two weeks of operation to 100 Ω (**Fig. 2B**) on the basis of polarization
174 measurements (revealing the significant reduction of internal resistance to this
175 order of magnitude). Phosphate buffer (50 mM, pH = 7) was used as catholyte
176 solution in this study. At the beginning, (80 mL) activated sludge collected from
177 the anaerobic pool of wastewater treatment plant (with pH adjusted to 7) was
178 filled to the anode chamber for inoculation. Information about the microbial
179 composition of the sludge can be found in our previous paper [35]. The rest of
180 the anolyte was phosphate buffer with Na-acetate as carbon source [22].
181 Acetate was dosed repeatedly in different amounts to ensure the actually
182 desired concentration (5 – 10 mM, **Fig. 2**). In each feeding cycles where the
183 acetate solution was loaded, the equivalent volume of spent media was drawn
184 before. Once the recorded voltage (closed-circuit potential difference between
185 the electrodes) dropped close to the initial, consecutive feeding was applied to
186 start the new experimental cycle.

187 The anode compartment was purged initially with nitrogen gas to
188 remove dissolved oxygen content. The anode and cathode chambers were
189 separated either by Nafion 115 PEM (Sigma-Aldrich, USA) or the SILM
190 membrane, both cut to circle shape with 8 cm diameter. The Nafion membrane
191 was pretreated before use as described by Ghasemi et al. [36]. The reactors
192 were placed in an incubator and operated under constant mesophilic
193 temperature of 35 °C. During CV measurements, an Ag/AgCl reference
194 electrode (filled with 3 M KCl solution) was inserted to the anode chamber of
195 the cells (more details on CV can be found in Section 2.3.4.).

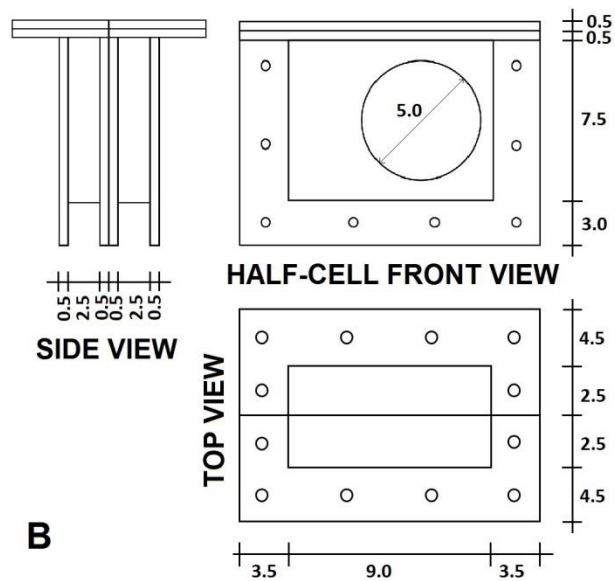
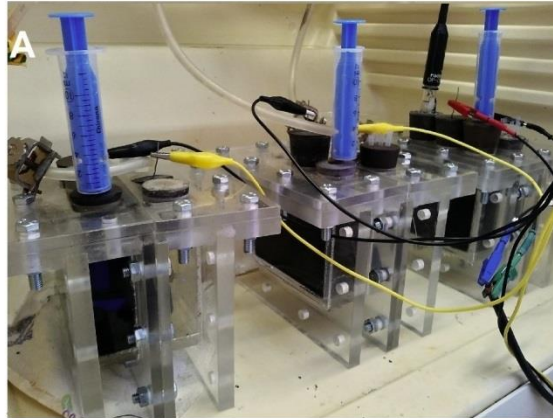


Fig. 1 – Image (A) and scheme (B) of the MFCs used in this study.

Dimensioning is in cm.

196

197

198

199

200 **2.3 Analysis and calculation**

201

202 **2.3.1. Calculations to report MFC efficiency**

203

204 The cell voltage was continuously registered by using a data acquisition
 205 device (National Instruments, USA). I and P were calculated based on Ohm's
 206 law (considering the actual value of external resistor applied in the circuit,
 207 Section 2.2.). From these data, I_d and P_d could be derived. Y_S , describing the
 208 MFCs from the point of view of energy recovery, was computed by Eq. 1 [34]).

209

$$Y_S = \frac{\int_0^{\tau} P(t) dt}{m(COD_{in}) A} \quad (1)$$

211

212 To evaluate charge utilization (reflected by the ratio of (i) the charge
213 successfully recovered in form of electricity and (ii) the charge contained in the
214 organic matter consumed), Coulombic efficiency was calculated according to
215 Eq. 2 [1].

216

$$CE = \frac{M \int I dt}{\Delta COD F V b} \quad (2)$$

218

219 where M is the molar mass of oxygen (g mol^{-1}), ΔCOD is the change in
220 chemical oxygen demand (g L^{-1}) during the process (COD was measured
221 according to standard methods), F is the Faraday's constant (96485 C mol^{-1}
222 electron), V is the total volume of the anolyte (L) and b is the number of
223 electrons exchanged per 1 mol of O_2 .

224

225 **2.3.2. Statistical analysis**

226

227 The statistical evaluation was carried out in Statistica 8 software to
228 compare MFCs operated with Nafion and SILM based on t-test (**Table 1**),
229 using the closed-circuit cell voltage data (as dependent variable), collected
230 over time for each stages indicated in **Fig. 2**.

231

232 **2.3.3. Dehydrogenase enzyme activity measurements**

233

234 Dehydrogenase enzyme activity was estimated based on the reduction
235 of TTC to TF [37]. In case of bulk samples, 1350 μl of Luria-Bertani medium
236 was mixed with 300 μl sample taken from the anolyte. Then, 150 μl TTC
237 reagent (5 g L^{-1}) was added to this mixture. In case of anodic samples, 2.2 x

238 0.5 x 0.2 cm pieces were cut off from the anode and put into the reaction
239 mixture. After 20 min of stirring at 200 rpm, 12 hours long incubation period at
240 37 °C was ensured [38]. Prior to extraction of formed TF by stirring the mixture
241 with 0.5 mL toluene at 200 rpm for 30 min, the reduction reaction was stopped
242 by injecting 100 µl of cc. sulfuric acid. Thereafter, the mixture in the Eppendorf
243 was centrifuged (4000 rpm, 5 min) and the toluene phase (supernatant) was
244 subjected to absorbance measurement at 492 nm using UV-VIS
245 spectrophotometer.

246

247 **2.3.4. Electrochemical techniques**

248

249 To derive fuel cell polarization curves, the external resistor was
250 sequentially changed from 47 kΩ down to 10 Ω and the potential difference
251 between anode and cathode electrodes was monitored after 20 min (provided
252 to reach the stabilization of potential signal under each condition). From the
253 linear range of the polarization curves (V vs. I) the value of R_i was determined
254 based on the slope of the fitted trendline. In addition, the maximal P_d values
255 were estimated considering the peak of the P_d vs. I_d plots.

256 CV was carried out by using a potentiostat (type: PalmSens 3,
257 PalmSens, Netherlands) in a three-electrode arrangement, where the anode
258 and cathode played the role of working and counter electrode, respectively,
259 meanwhile an Ag/AgCl electrode (placed in the anode chamber and filled with
260 3 M KCl solution) was used as reference electrode. It is noteworthy that all
261 electrode potential values reported in this paper are given with respect to
262 Ag/AgCl (3 M KCl) reference electrode. CV measurements were conducted
263 under non-turnover conditions at different stages of MFC operation (three
264 times in each condition, accepting the third scan to be representative). The
265 voltammograms were recorded by using 1 mV s⁻¹ scan rate between +0.25 V
266 and -0.65 V anode potentials (vs. Ag/AgCl, 3 M KCl), unless otherwise stated.

267 EIS measurements were carried out by using the impedance analysis
268 function of the combined potentiostat (PalmSens 3, PalmSens, Netherlands) in

269 a whole-cell experimental setup (two-electrode arrangement), where the
270 working electrode was the anode and the cathode served as both counter and
271 reference electrodes. AC amplitude of 10 mV and frequency range of 50 kHz –
272 1 MHz were used. The measurements were conducted in presence of acetate
273 substrate during the maximal electricity producing stage of the MFCs under
274 open circuit operating mode (established two hours before EIS analysis).
275 Equivalent circuit model fitting was carried out in EIS Spectrum Analyser
276 software (ABC Chemistry).

277

278 **3. Results and Discussion**

279

280 **3.1. Voltage profiles and current generation in response to different** 281 **acetate supplementations**

282

283 Once the cells were assembled, measurements and acquisition of data
284 were started. During the acclimation period, varied amounts of acetate
285 substrate were fed in subsequent batch cycles as indicated by arrows in **Fig.**
286 **2A**. After inoculation, as the start-up period commenced (no acetate feeding,
287 **Fig. 2A**, first cycle), all MFCs showed quite low voltage outputs but the
288 tendencies were different. On the one hand, almost prompt current generation
289 was noted in case of PEM-MFC and after reaching a peak value, I_d remained
290 around 51 mA m⁻². On the other hand, the ILM-MFC began to produce
291 electricity less instantly (after a half-day) with a maximum I_d of about 63 mA m⁻
292 ². Overall, in this period, in accordance with the statistical analysis in **Table 1**,
293 PEM-MFC generated significantly higher average voltages than ILM-MFC did
294 (**Table 1**).

Table 1 – Statistical analysis of voltages produced in MFCs operated with PEM and SILM

Dependent variable: Closed-circuit voltage (mV)	Mean (PEM)	Mean (SILM)	t-value	df	p-value	Valid N (PEM)	Valid N (SILM)	Std. Dev. (PEM)	Std. Dev. (SILM)
no acetate feeding (Fig. 2A first cycle)	126.616	78.750	7.372	170	<0.001	86	86	16.383	57.939
5 mM acetate feeding (Fig. 2A second cycle)	223.354	191.196	5.355	214	<0.001	108	108	38.455	49.160
10 mM acetate feeding (Fig. 2A third cycle)	300.029	312.595	-2.416	520	0.016	261	261	71.549	44.043
5 mM acetate feeding (Fig. 2A fourth cycle)	241.715	277.429	-5.162	352	<0.001	177	177	60.960	68.974
7.5 mM acetate feeding (Fig. 2B first cycle)	85.459	107.727	-5.794	318	<0.001	177	143	20.008	46.044
5 mM acetate feeding (Fig. 2B second cycle)	61.190	97.097	-10.099	281	<0.001	140	143	20.424	36.898
6 mM acetate feeding (Fig. 2B third cycle)	66.252	108.159	-13.565	283	<0.001	149	136	8.166	36.735

p < 0.05 indicates statistical significance

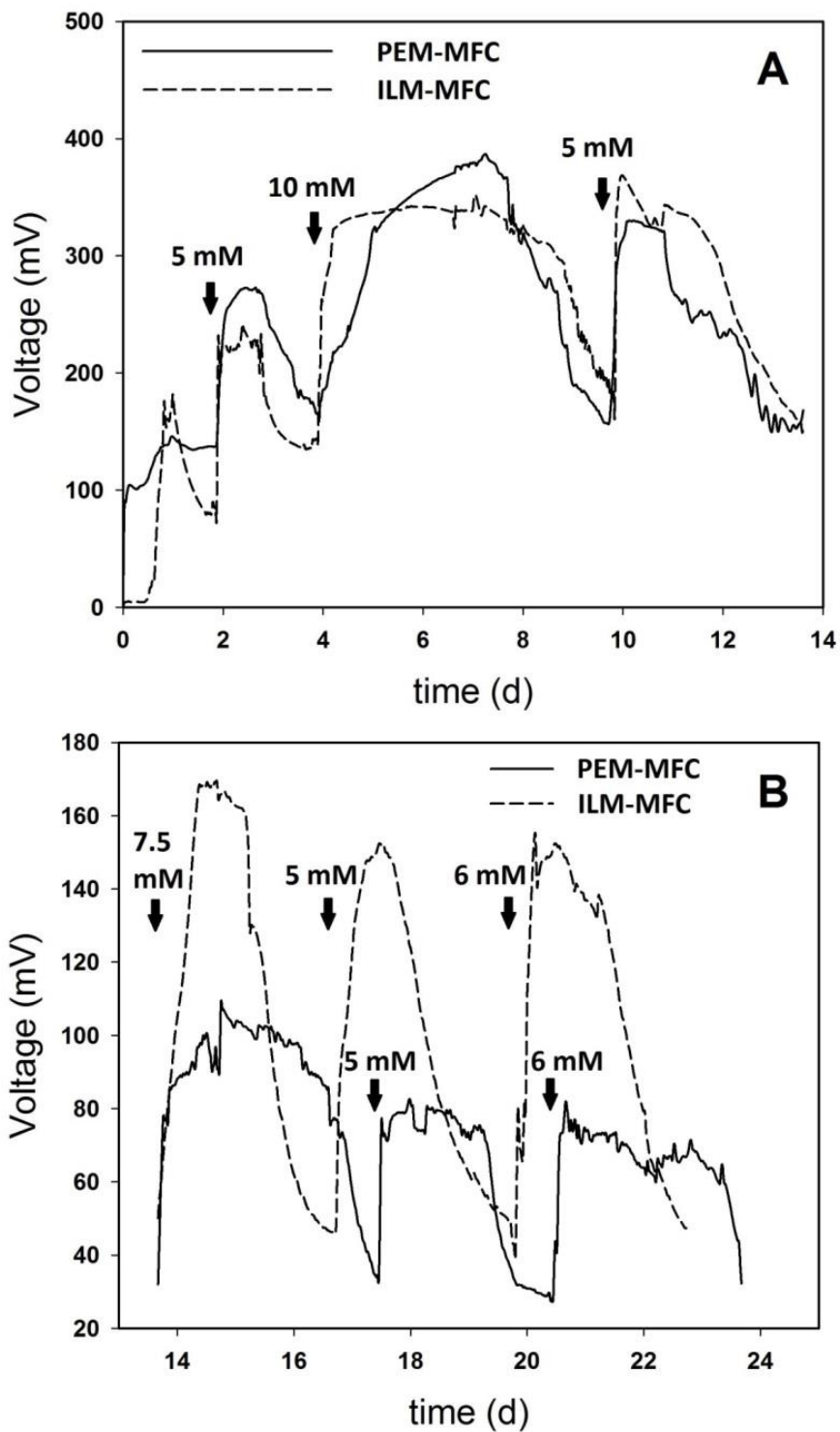
positive t-value means that PEM performs better than SILM, while negative t-value presents the opposite case

296 After 2 days, the first dose of acetate was injected (**Fig. 2A**, second
297 cycle) to ensure 5 mM concentration in the anode compartment. As a result,
298 quick response could be observed after this organic matter loading in both
299 systems. Still, the PEM-MFC reflected statistically higher voltages (**Table 1**),
300 reaching 102 mA m⁻² as highest current density. In the meantime, peak I_d of 88
301 mA m⁻² was registered for the ILM-MFC. As it can be also seen in **Fig. 2A**
302 (third cycle), the 10 mM acetate induced proportionally higher voltage and
303 current density (compared to previous stage with 5 mM), peaking at 385 mV
304 and corresponding 148 mA m⁻² for PEM-MFC, whilst at 342 mV and 131 mA
305 m⁻² for ILM-MFC. It is noteworthy that in this period and onwards (**Table 1**), the
306 ILM-MFC outperformed the PEM-MFC.

307 Moreover, it is important to notice the significantly different outcomes of
308 the first and second 5 mM acetate additions (**Fig. 2A**, second and fourth
309 cycles), which imply the proper and gradual development of the
310 electrochemically-active populations. Actually, the extent of current density
311 increase was clearly distinguishable for the reactors employing the two
312 different separators. For instance, in case of MFCs equipped with PEM, the
313 increment was nearly 30 % (133 mA m⁻² vs. 102 mA m⁻²), while for ILM-MFC,
314 the 152 mA m⁻² realized in the fourth cycle (**Fig. 2A**) represented a more than
315 72 % enhancement relative to the second cycle. Consequently, in this term,
316 the bioelectrochemical system installed with SILM was capable to remarkably
317 outperform its counterpart with Nafion.

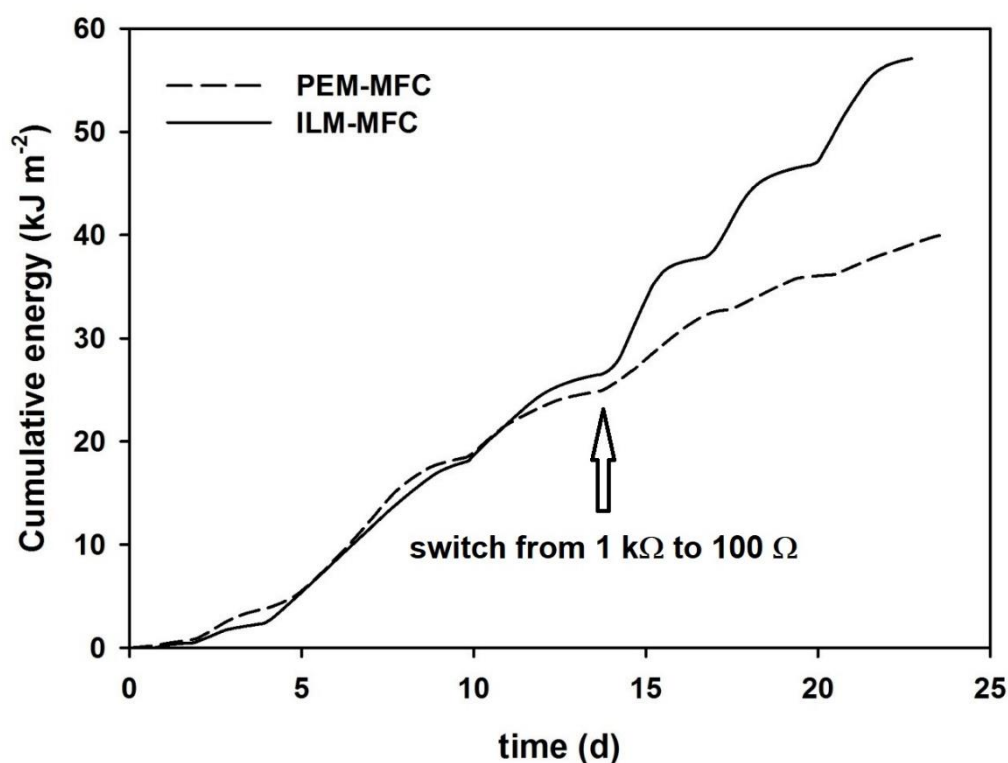
318 As mentioned in Section 2.2., at the point of the 4th substrate injection
319 (**Fig. 2B**, first cycle), the external resistor was changed from 1 k Ω to 100 Ω in
320 both ILM-MFC and PEM-MFC, because of the feedback received from cell
321 polarization measurements (elaborated later on in Section 3.5.) indicating the
322 change of total internal resistances over time. As a result, differences in the
323 efficiency of the two systems became even more remarkable. In particular, as
324 it can be seen in **Fig. 2B**, the highest voltages and thus, maximum current
325 densities were considerably better for ILM-MFC, i.e. 739, 656 and 695 mA m⁻²

326 compared to 461, 348 and 373 mA m⁻² generated by PEM-MFC at 7.5, 5 and 6
327 mM acetate concentrations, respectively.



328
329 **Fig. 2** – Voltage profiles of MFCs equipped with different membranes.
330 Measurements at various acetate concentrations (A) $R_i = 1 \text{ k}\Omega$ and (B) $R_i =$
331 100Ω .

332 The total (cumulative) energy recovery (normalized to the anode surface area)
333 is illustrated in **Fig. 3**. It can be seen that though PEM-MFC was more
334 effective in generating electrical energy for the two initial feeding cycles
335 (reflected also by the significantly higher, mean voltage values presented in
336 **Table 2**), the ILM-MFC could take over with time (from the 3rd substrate
337 addition and onwards) and perform in a considerably better way.



338
339 **Fig. 3** – Cumulative energy production of MFCs equipped with different
340 membranes under conditions displayed in **Fig. 2**.

341
342 At this point, besides the evaluation presented so far, we feel important
343 to comment on process stability, which can be challenging when a supported
344 ionic liquid membrane is used. In SILMs, the IL stays in the pores of
345 supporting material thanks mainly to capillary forces, which is influenced by
346 factors e.g. the viscosity of IL [39]. In addition, the compatibility of IL and the
347 support membrane can affect consistent SILM performance as well as the
348 formation of water microenvironments inside the IL phase [39].

349 In this aspect, as discussed by Fortunato et al. [40], the loss of
350 immobilized liquid from the pores (in case of supported liquid membranes) can
351 potentially be mitigated by the appropriate selection of the phase properties in
352 contact, in particular the membrane and the solution around it. During SILM
353 fabrication, for a given support matrix in which the IL is filled, the membrane
354 traits can eventually be adjusted by the choice of IL, where the molecular
355 structures of anion and cation (building up the IL) will play a significant role. If
356 the purpose is the use of SILM in an aqueous media such as in MFCs (where
357 anolyte as well as catholyte are water-based solutions) hydrophobic, room-
358 temperature ILs may be more appropriate in order to reduce miscibility and
359 consequently, the threat of possible leaching of IL from the membrane pores.
360 In general, hydrophobicity of ILs with an imidazolium-type cation ($[C_n\text{mim}]^+$)
361 increases with the length of alkyl side-chain and moreover, the anion ($[X]^-$)
362 properties i.e. $[\text{NTf}_2]^-$ vs. $[\text{PF}_6]^-$ will also take an effect [41].

363 As a matter of fact, Fortunato et al. [42] investigated the durability of
364 SILMs prepared with ILs of the imidazolium family i.e. $[\text{bmim}][\text{PF}_6]$ and PVDF
365 support membrane, similar to this study. In essence, it was reported that such
366 SILMs could preserve their hydrophobic characteristic after contacted with
367 water and furthermore, no considerable displacement of IL from the pores
368 could be noted as long as mild stirring conditions were maintained.
369 Additionally, in the continuation of that work [40], it was demonstrated that
370 even if the concentration of imidazolium-type IL in the aqueous phase
371 surrounding the SILM rose under dynamic (e.g. intensely stirred)
372 circumstances, it was primarily originated from the rinsing of excess IL located
373 on the membrane surface rather than from displacing the IL from the
374 membrane pores.

375 On the grounds of these arguments and taking into account that no
376 stirring was directly provided in the MFCs of this investigation – representing
377 more or less static conditions on two, anode- and cathode-facing sides of the
378 SILM (though continuous air supply in the cathode chamber may have had
379 some inherent contribution here) – it may be supposed that SILMs

380 manufactured by embedding [bmim][PF₆] in microfiltration PVDF membrane
381 could be considered stable enough. As a result, this SILM may be seen as a
382 plausible candidate withstanding longer-term MFC operation, which is implied
383 also by the outcomes of 3-4 weeks of experimentation lacking any membrane-
384 associated failures (**Fig. 2**). Nevertheless, to strengthen these assumptions
385 and conclusions, a future study can be proposed.

386 A further investigation on SILM stability and application can be also
387 useful to take a look into process safety. On the one hand, from previous
388 studies such as [Nemestóthy et al. \[43\]](#), it seems that ILs might act as inhibitors
389 in anaerobic fermentation systems, depending on the IL type and
390 concentration. Therefore, if leakage of ILs from the SILM occurs over time, it
391 may cause challenges to keep the electro-active bacteria in good conditions
392 and maintain sufficient process performance. However, this aspect should be
393 examined case-specifically for the actual underlying microbial community,
394 which, thanks to the wide range of inocula used by researchers, can be quite
395 different from one MFC to another. On the other hand, nevertheless, [Jebur et al. \[44\]](#)
396 have found that membranes prepared with ionic liquid can have anti-
397 microbial impact and in that way, suppress the undesired biofouling of the
398 separator. Such a property could deserve attention since fouling of
399 membranes in bioelectrochemical systems can lead to severe operational
400 issues.

401

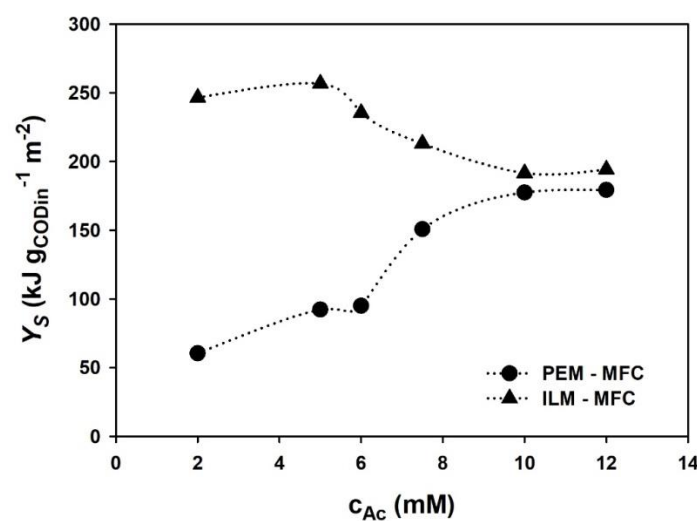
402 **3.2. Evaluation of bioelectrochemical cell performance applying ionic** 403 **liquid-containing and Nafion membrane separators**

404

405 The efficiency parameters (for instance substrate removal, Coulombic
406 efficiency, energy yield, etc.) of microbial electrochemical systems are usually
407 dependent on the operating conditions [\[1, 13\]](#), among which substrate
408 concentration is one of the most important [\[45\]](#). For instance, it has been
409 previously found that ILM-MFCs were able to reach higher energy yields at low
410 acetate concentrations than those relying on Nafion [\[33\]](#). Hence, besides the

411 acetate loadings tested and discussed in Section 3.1., complementary
412 measurements along with additional substrate concentrations were carried out
413 and the dependency of Y_S on this process variable was assessed in MFCs
414 employing SILM or Nafion membrane. Overall, the 6 initial acetate
415 concentrations set in the anode chamber were as follows: 2, 5, 6, 7.5, 10 and
416 12 mM.

417 The results are illustrated in **Fig. 4**, where it is to observe that the energy
418 yield values were significantly enhanced between 2 – 7.5 mM substrate
419 concentrations (approximately 4x, 3x, 2.6x and 1.4x higher for 2, 5, 6 and 7.5
420 mM acetate, respectively) in case of ILM-MFC compared to PEM-MFC. At
421 higher acetate concentrations (10 and 7.5 mM), the differences between the
422 two cells became much smaller, but Y_S was still somewhat higher for the ILM-
423 MFC. This may suggest that under such substrate loadings, the metabolic
424 (substrate-utilizing) capacity of exoelectrogenic microorganisms in both MFCs
425 reached an upper-bound. Besides, the potential presence of methanogenic
426 *archaea* (occurring in the mesophilic, anaerobic sludge applied for inoculation)
427 should be also taken into account. This could affect the total energy recovery
428 via microbiological competition for the organic matter. This phenomenon can
429 be a possible threat at increased substrate availability [46].



430

431 **Fig. 4** – Y_S as a function of acetate concentration. c_{Ac} represents initial acetate
432 concentrations in the anode chamber.

433 The largest Y_S was realized in the ILM-MFC ($Y_S = 256.8 \text{ kJ g}_{\text{COD,in}}^{-1} \text{ m}^{-2}$
434 at 5 mM acetate concentration), while $180 \text{ kJ g}_{\text{COD,in}}^{-1} \text{ m}^{-2}$ could be achieved in
435 the MFC using the Nafion proton exchange membrane (at 12 mM acetate
436 concentration).

437 To evaluate the utilization of electrons (released from organic matter
438 degradation) in MFCs, the Coulombic efficiency was determined at 6 mM
439 acetate addition (last cycle in **Fig. 2B**). In fact, CE of $13.9 \pm 0.4 \%$ and $24.0 \pm$
440 0.7% could be attained for the PEM-MFC and ILM-MFC, respectively.
441 Therefore, from this point of view, the application of SILM resulted in a more
442 attractive bioelectrochemical process. As for the alteration of CE in the
443 function of substrate concentration, a decreasing tendency was presented by
444 [Sleutels et al. \[47\]](#) within an acetate influent concentration range of 1 – 35 mM.
445 This is in good agreement with the findings of our previous [\[33\]](#) and present
446 studies, suggesting the use of low acetate concentrations in order to support
447 higher specific energy recoveries (**Fig. 4**).

448 In summary, the experiments revealed the positive impact of SILM on
449 both energy yield (especially at low substrate concentrations) and Coulombic
450 efficiency. In addition, it turned out that the hydrophobic [bmim][PF₆]-based
451 SILM can be used properly for separating the electrode chambers in two-
452 compartment MFCs to produce electricity with an effectiveness more or less
453 comparable to Nafion when higher substrate loadings are applied.
454 Nevertheless, to dissect the possible contribution of membranes in the MFC'
455 behaviors and facilitate the understanding of the process, further tests e.g. (i)
456 cell polarization, (ii) monitoring of dehydrogenase enzyme activity as well as
457 (iii) cyclic voltammetry were performed and are discussed in the next sections.

458

459 **3.3. Analysis of MFC behavior via polarization measurements**

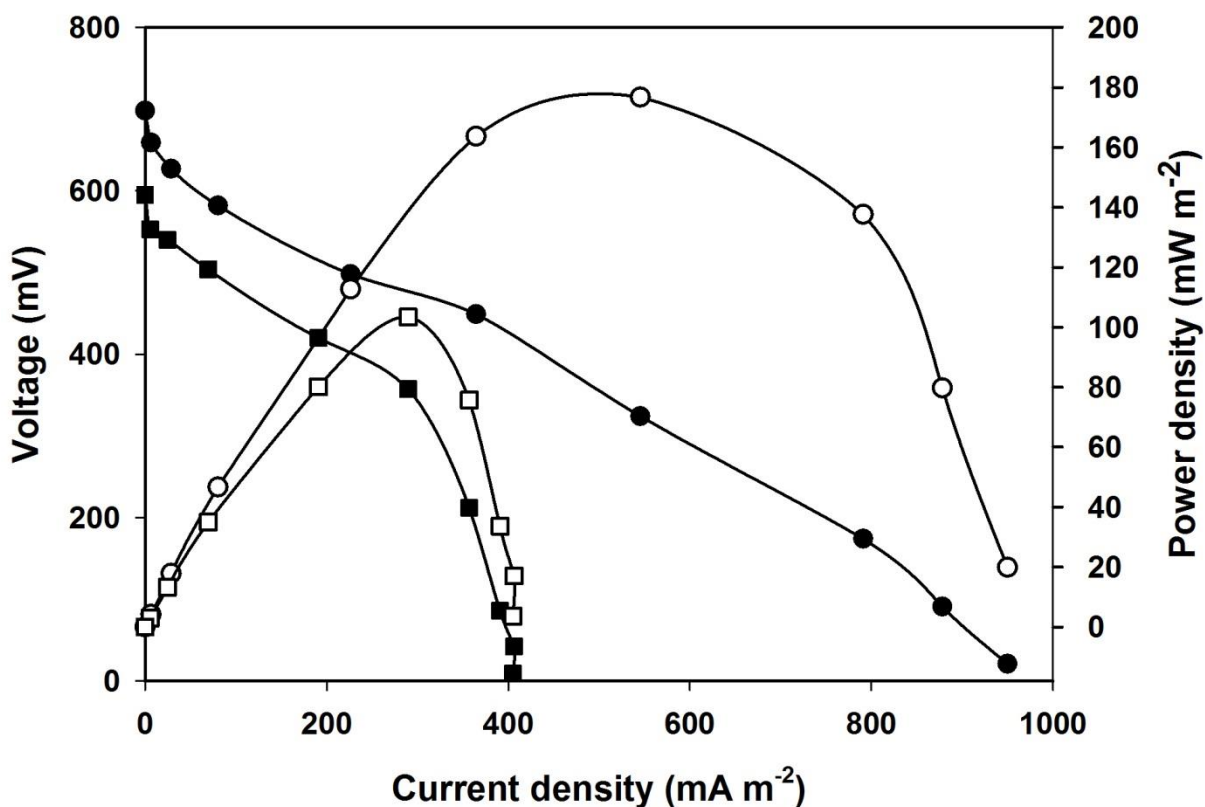
460

461 The cell polarization measurements assist the calculation of R_i for MFCs
462 and hence, help the selection of appropriate R_e by which P_d is enhanced.
463 Under the condition then $R_i = R_e$, the CDP of MFC is reached [\[48\]](#).

464 On the third day after inoculation, R_i values were found to be $581 \pm 11 \Omega$
465 and $789 \pm 9 \Omega$ for ILM-MFC and PEM-MFC, respectively. Besides, estimated
466 power densities at CDP were $39.8 \pm 2.7 \text{ mW m}^{-2}$ and $78.0 \pm 3.1 \text{ mW m}^{-2}$,
467 respectively. After two weeks, R_i values decreased considerably in both
468 systems to $276 \pm 16 \Omega$ and $303 \pm 11 \Omega$, respectively. The approximate
469 maximum power densities at CDP were as high as $190.1 \pm 9 \text{ mW m}^{-2}$ and 98.6
470 $\pm 11.6 \text{ mW m}^{-2}$ in case of ILM-MFC and PEM-MFC. The observed tendency
471 during the first 14 days for R_i supports the conclusions of Section 3.1. pertain
472 to the development of the MFCs reflected by current density outputs.
473 Polarization measurements were continued and after three weeks, almost no
474 additional change of R_i ($268 \pm 11 \Omega$ and $302 \pm 17 \Omega$ for ILM-MFC and PEM-
475 MFC, respectively) could be noted. Consequently, stabilization of maximal
476 power densities was attained and the microbial fuel cells were considered as
477 adapted systems (**Fig. 5**).

478 Basically, the characteristics of polarization (**Fig. 5**) curves are similar to
479 those found in the relevant literature [23, 34, 49], showing a declining pattern
480 in current density along with increased R_e . Furthermore, the absence of power
481 overshoot is good indication of appropriate bioelectrochemical system
482 operation [17]. Moreover, it is to infer that the MFCs employing the SILM not
483 only achieved lower R_i but at the same time, ensured > 70 % higher maximal
484 power density ($500 \pm 21 \text{ mA m}^{-2}$ of I_d vs. $290 \pm 19 \text{ mA m}^{-2}$ for PEM-MFC) at
485 CDP. The maximal $950 \pm 84 \text{ mA m}^{-2}$ of I_d (vs. $405 \pm 30 \text{ mA m}^{-2}$ for PEM-MFC)
486 was accomplished with the lowest resistance (10Ω), presumably because of
487 effective electron discharge [49].

488 In this polarization study, voltage drop was more significant for PEM-
489 MFC within the concentration polarization range (at high current density). It is
490 a probable signal of more pronounced increase in the ratio of oxidized and
491 reduced charge-shuttling molecules (being at different redox state) in the
492 vicinity of electrode surface [1]. This assumed phenomena can be ascribed to
493 the limited discharge of reduced or supply of oxidized compounds, leading to
494 higher anode potentials or on the contrary, lower potentials at the cathode [1].



495

496 **Fig. 5** – Polarization curves for (●) ILM-MFC and (■) PEM-MFC and power
 497 density plots for (○) ILM-MFC and (□) PEM-MFC (taken on the 21st day, 6 mM
 498 acetate)

499

500 It is important to mention that the attractiveness of membranes for MFCs
 501 should be assessed under the similar settings/combination of environmental
 502 factors [17] such as in terms of seed source, substrate quality, electrode
 503 materials, anode/cathode potential(s) and spacing, anolyte/catholyte solution
 504 traits i.e. conductivity, physiological conditions i.e. temperature, pH, etc.
 505 otherwise, it is difficult to say which system and in particular, which membrane
 506 is more suitable than another [50]. Nonetheless, in general, MFCs are capable
 507 of producing power densities both above and below the values reported in the
 508 present work (**Table 2**). Similar conclusions can be made on the grounds of
 509 the analysis carried out by Ge et al. [51], where it was clearly reported that

510 MFC power densities can span a wide range (through order of magnitudes),
 511 fitting our results obtained both with the IL-containing and Nafion membranes.

512

513 **Table 2 – Comparative table with literature data. The power density data**
 514 **marked with (*) are given as granular anode volume specific values**

515

MFC type	Membrane	Power density (mW m ⁻² / mW m ⁻³ *)	Internal resistance (Ω)	Substrate	Reference
Dual-chamber MFC	Nafion (3.5, 6.2 and 30.6 cm ²)	44 - 173	1110 – 89.2	Acetate	[23]
Dual-chamber MFC	Nafion (~20 cm ²)	51 – 67.5	300 - 500	Synthetic wastewater	[53]
Single-chamber MFC	[omim][PF ₆]- PVC	45*	4500 – 5900		
Single-chamber MFC	[mtoa][Cl]- PVC	450*	440 - 750	Brewery wastewater	[54]
Dual-chamber MFC	Nafion	100*	2000		
Dual-chamber MFC	[hmim][PF ₆]	3.7	2900		
Dual-chamber MFC	[bmim][NTf ₂]	3.9	2500	Acetate	[34]
Dual-chamber MFC	Nafion	12.2	1350		
Dual-chamber MFC	[bmim][PF ₆]	179	268		
Dual-chamber MFC	Nafion	101	302	Acetate	This study

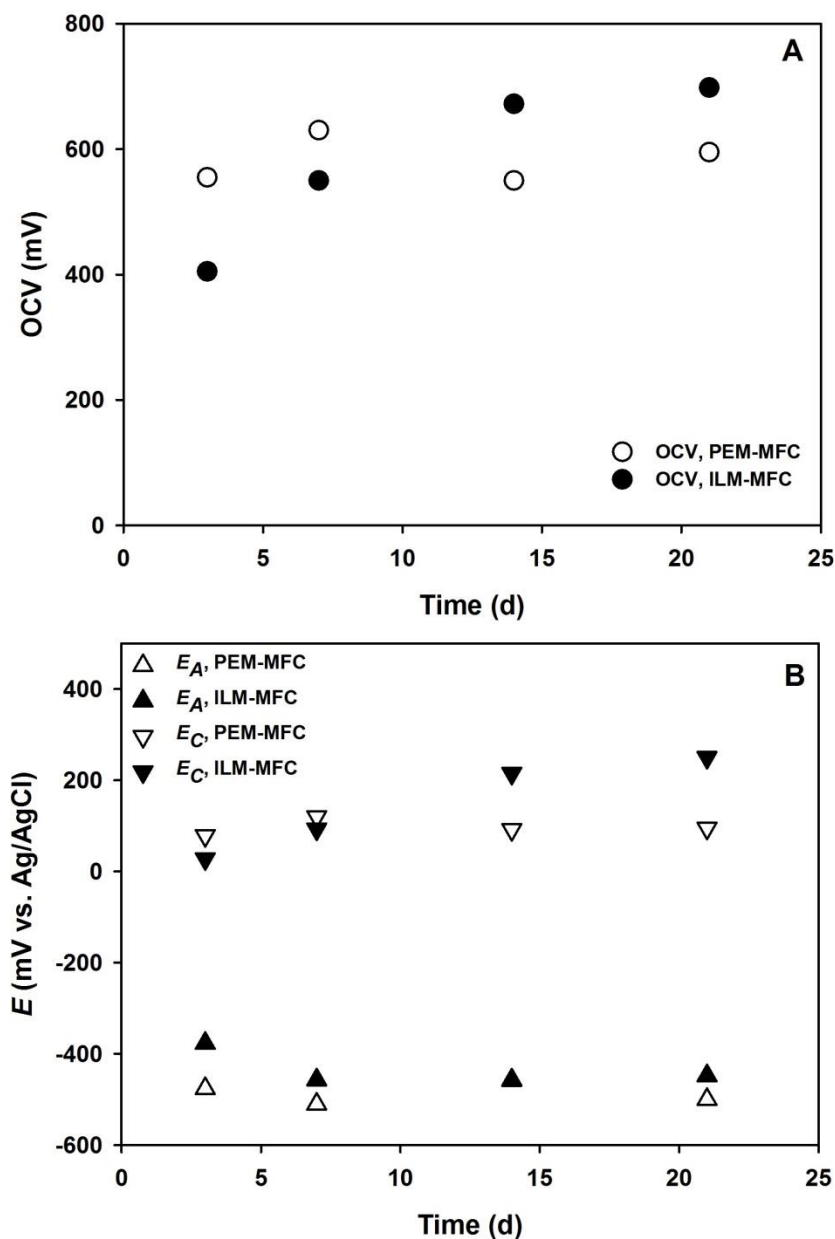
516

517 **3.4. Alteration of electrode potentials in MFCs equipped with SILM or**
518 **Nafion membrane**

519

520 By monitoring both the individual anode and cathode potentials (and the
521 difference between those values), information about the potential losses
522 occurring in the system can be extracted and beside, the assignment of these
523 losses to given processes (e. g. electrode reaction or diffusive transport, etc.)
524 may be possible.

525 Considering the OCV of MFCs during acetate utilization (**Fig. 6A**), a
526 strictly monotonic increase could be observed as a function of elapsed time in
527 case of ILM-MFC, from 405 mV (on 3rd day) up to 698 mV (on 21st day). For
528 PEM-MFC, however, such a trend could not be detected and rather, a nearly
529 steady OCV (around 583 mV) was obtained. The determination of
530 accompanying anode and cathode potentials revealed quite comparable
531 values in the two systems: $E_a = -452 \pm 5$ mV and $E_a = -485 \pm 25$ mV in case
532 of ILM-MFC and PEM-MFC, respectively. Nevertheless, the alteration of E_c
533 with time in the two MFCs (assembled with various membrane separators)
534 was more distinguishable. In ILM-MFC, change of E_c followed a similar pattern
535 than respective OCV (**Fig. 6B**), resulting in an increment from +28 mV (3rd
536 day) to +250 mV (on 21st day). As for PEM-MFC, E_c was found to be relatively
537 higher at the early stage of operation ($E_c = +79$ mV, 3rd day) and rose to +120
538 mV on the 7th day. From that point onwards (14th and 21st days in **Fig. 6B**), a
539 stabilized value ($+93 \pm 2$ mV) could be measured.



540
 541 **Fig. 6** – OCV (A) and electrode potentials (B) of the MFCs measured at
 542 maximal current density stages.

543
 544 These phenomena imply the importance of the membrane separator
 545 type, which seemed to be a responsible factor for the registered changes of
 546 electrode potentials, in particular E_c . As a matter of fact, the transport of
 547 certain cations (e.g. Na^+ and K^+) may affect the migration of protons from the
 548 anode to the cathode, causing potentially a pH split due to H^+ accumulation in
 549 the anode chamber [19]. Hence, the passage of those ions through the

550 membrane presents an issue to deal with and can be associated with
551 structural properties of the membrane material [19] since, for instance, the
552 sulfonate groups of Nafion can get occupied by the above mentioned cationic
553 species [21, 55, 56]. Additionally, problems related with the time-stability i.e.
554 due to (bio)fouling of Nafion may arise [57]. In contrast, the SILM (based on
555 [bmim][PF₆] ionic liquid and PVDF as supporting membrane layer, which would
556 appear as a feasible separator candidate to improve (i) energy yields, (ii)
557 current and power densities and (iii) lower cathodic losses – has several
558 underexplored characteristics at the moment, including mechanism of H⁺
559 transport and selectivity to transfer various compounds in the anolyte and
560 catholyte (cross-over effect). In the light of that, the mechanism of ion transfer
561 through ILs having special physico-chemical properties is one crucial aspect to
562 be elaborated and compared to polymer membranes such as Nafion.
563 Nonetheless, as it has been recently communicated in our previous paper [34],
564 the SILMs can have lower O₂ mass transfer coefficients and one order of
565 magnitude lower transport rate for acetate ion (referred as substrate cross-
566 over), which can be another relevant information to take into account from a
567 process evaluation point of view.

568

569 **3.5. Assessment of SILM- and Nafion-dependent MFC behaviors by** 570 **dehydrogenase activity monitoring**

571

572 To further elucidate the observed differences in the behavior of MFCs
573 assembled with various membrane separators, feedback from a biological
574 activity viewpoint can be useful (i.e. the production of charge carriers is
575 primarily attached to strain metabolism) [58]. Measurements on
576 dehydrogenase enzyme are able to characterize the metabolism-related
577 microbial redox activity, since this intracellular biocatalyst plays an important
578 role on H⁺ (and coupled e⁻) transfer between metabolites and indirectly (by
579 ensuring accessible charges and using redox mediators) on the maintenance
580 of electron driving force [38].

581 In our system, samples taken from the bulk phase as well as from the
582 anode (biofilm) were analyzed according to Section 2.3.3. In the former case,
583 for both ILM-MFC and PEM-MFC, a progressively decreasing tendency was
584 shown as the systems approached stable operation (**Table 3**).

585

586 **Table 3 – Results of dehydrogenase activity measurements of bulk**
587 **samples taken at different stages of system development**

588

	DA ($\mu\text{g mL}^{-1}$ of toluene)	
	PEM-MFC	ILM-MFC
Day 3	20.77	15.8
Day 7	4.07	8.15
Day 21	2.82	3.27

589

590 This could be an indicator of lowered metabolic redox activity in the
591 liquid surrounding the anode electrode [38]. This seems to be reasonable
592 since in an MFC system, the proper development of an electro-active biofilm
593 on the anode surface should be accompanied by the suppression of planktonic
594 cells [59]. These results coincide well with the literature, where, for instance,
595 DA over time was investigated by Reddy et al. [38] in single chamber MFCs at
596 different organic loading rates. In brief, initial increase from 9 up to 18 $\mu\text{g mL}^{-1}$
597 toluene (until $\sim 12^{\text{th}}$ hour) and a consecutive decrease down to 2 – 4 $\mu\text{g mL}^{-1}$
598 toluene were demonstrated for samples withdrawn from the anolyte
599 (containing the suspended/planktonic cells).

600 In contrast, higher DA could be presumed in case of anodic samples
601 because of the enrichment of active, anodophilic strains and indeed,
602 supporting experimental results were obtained (**Table 3**). On the 3rd day, the
603 anodic DA values were somewhat similar, i.e. 1.23 $\mu\text{g mL}^{-1}$ toluene and 1.15
604 $\mu\text{g mL}^{-1}$ toluene for the PEM-MFC and ILM-MFC, respectively. Later on (in

605 parallel with the evolution of current described in Section 3.1.), the DA data (in
 606 both MFC systems) reflected rising tendencies with time. In case of ILM-MFC,
 607 values determined on the 7th and 21st days were 5.77 $\mu\text{g mL}^{-1}$ toluene and
 608 8.04 $\mu\text{g mL}^{-1}$ toluene. For PEM-MFC, respective DAs were found as 3.33 μg
 609 mL^{-1} toluene and 6.11 $\mu\text{g mL}^{-1}$ toluene (**Table 4**).

610

611 **Table 4 – Results of dehydrogenase activity measurements of anode**
 612 **samples taken at different stages of system development**

613

	DA ($\mu\text{g mL}^{-1}$ of toluene)	
	PEM-MFC	ILM-MFC
Day 3	1.23	1.15
Day 7	3.33	5.77
Day 14	3.84	7.02
Day 21	6.11	8.04

614

615 To evaluate the likely positive effect of SILM on anode-related DA
 616 compared to PEM-MFC (indicated by the differences in DA), various mass
 617 transport phenomena (that may affect the microbial redox metabolism) taking
 618 place across the membrane should be considered. In agreement with the
 619 statements made above, SILMs can have lower oxygen transfer rate relative to
 620 Nafion, as communicated in our recent work using [bmim][NTf₂] ionic liquid
 621 [34]. This property could be helpful to more successfully protect the anode
 622 chamber from oxygen gas penetration and therefore, maintain anoxic
 623 conditions. In MFCs, it is a requirement to keep the anaerobic
 624 (electrochemically-active) microbes in good conditions and prevent metabolic
 625 shifts, which may occur once terminal electron acceptors (such as oxygen)
 626 other than the anode material itself are available for cell respiration. In
 627 addition, SILMs (compared to Nafion) can have the potential to act as effective
 628 barriers and reduce substrate-related losses linked to cross-over effect [34].
 629 Faster transport of substrate towards the cathode chamber may result in

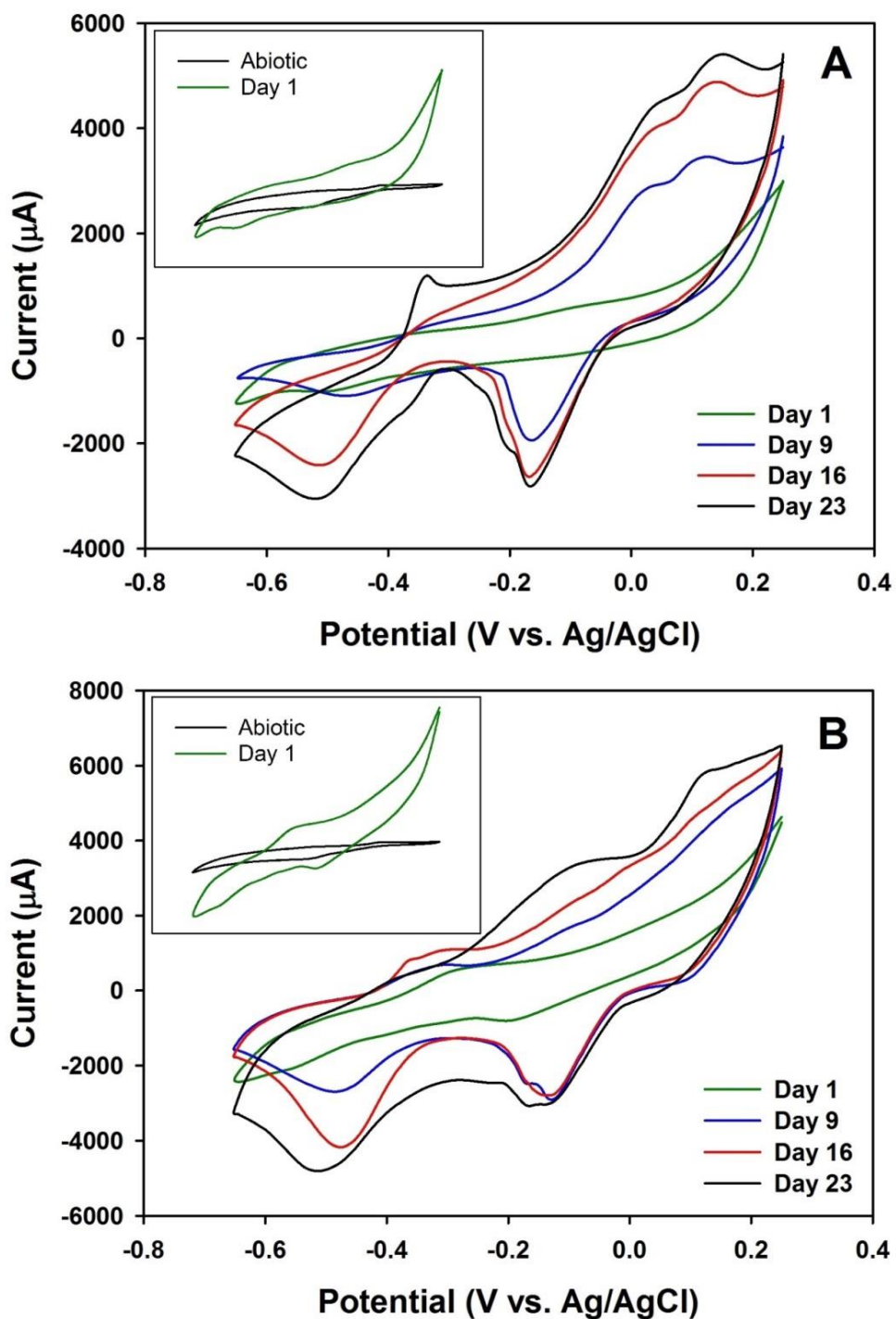
630 relatively lowered anode-side substrate concentration, which may limit the
631 redox activity of microorganisms. Mainly, this issue can occur at initially low
632 substrate concentrations, which was the case of the present study.

633

634 **3.6. Cyclic voltammetric analysis of MFCs operated with SILM and Nafion** 635 **membranes**

636

637 In general, as discussed in Section 3.5., DA gives insight to the
638 metabolic redox activity of particular microbial communities i.e. those located
639 and growing on the anode [38]. Nonetheless, in order to characterize the
640 electrochemically-active population itself, cyclic voltammetry (CV) can be
641 proposed [60, 61]. The cyclic voltammograms in **Figs. 7A and B** revealed
642 several oxidation-reduction peaks in both ILM- and PEM-MFCs and
643 furthermore, suggest the dynamic variation of electrocatalytic activity on
644 anodes, irrespective of the membrane used. Actually, the increase of detected
645 peak currents over time indicate (i) the enrichment of redox mediators and/or
646 (ii) larger coverage of anode by proteins involved in the electron transfer
647 process [62]. Notwithstanding, a comprehensive approach is required when it
648 is aimed to fairly compare various bioelectrochemically active systems based
649 on the quantification of the above-mentioned mediators and/or proteins taking
650 part in the electron transfer due to the commonly occurring lack of information
651 about the actual bacterial concentrations [61, 63]. This appears to be the case
652 in our MFCs as certain conditions were not identical for example in terms of
653 anolyte properties such as ion and cell concentrations, which can be
654 associated with the employment of membranes and their mass transport
655 features.



656
 657 **Fig. 7** – Cyclic voltammograms recorded at scan rate of 1 mV s^{-1} under non-
 658 turnover (under acetate substrate depleted). conditions: (A) ILM-MFC; (B)
 659 PEM-MFC.

660
 661 Nonetheless, even under such conditions, the assessment of changes in
 662 each individual MFC can be performed. For instance, in **Fig. 7A**, a complex

663 redox behavior of ILM-MFC anode can be seen. The voltammogram (recorded
664 on the 1st day) implied the existence of a weak reduction peak at -0.51 V
665 (corresponding peak current: 1 mA) in the reverse scan, while no redox peaks
666 could be detected for the virgin anode. After 9 days of operation, weak
667 oxidation peaks were spotted at about (i) -0.35 V (corresponding peak current:
668 0.25 mA), (ii) $+0.03$ V (corresponding peak current: 2.8 mA) and (iii) $+0.16$ V
669 (corresponding peak current: 3.5 mA) in the forward scan and at the same
670 time, reduction peaks appeared at (iv) -0.18 V (corresponding peak current: 2
671 mA), (v) -0.47 V (corresponding peak current: 1 mA) in the reverse direction. In
672 accordance with **Fig. 7A**, it can be stated that the peak currents increased
673 over time and moreover, on the 23rd day, two overlapping peaks were found at
674 about -0.18 V and -0.2 V (3 mA and 2.1 mA). Overall, on the 23rd day, the
675 anode of ILM-MFC could be characterized by (at least) three well-
676 distinguishable redox systems.

677 Considering the CVs of PEM-MFC (**Fig. 7B**), no redox activity in case of
678 virgin anode was observable, just like for ILM-MFC. Afterwards, on the 1st day,
679 weak oxidation (-0.29 V) and reduction (-0.2 V) peaks appeared, with peak
680 currents of about 0.3 mA and 1 mA, respectively. Similar to ILM-MFCs, the
681 redox current peaks of the bioelectrochemical system equipped with Nafion
682 membrane increased as a function of operation time, resulting also in (at least)
683 three active redox components (**Fig. 7B**). In summary, slight differences could
684 be identified in terms of the (i) oxidation peaks in the forward scan and (ii) the
685 absolute values of peak currents, compared to ILM-MFC.

686 Thereafter, additional CV measurements were carried out by adjusting
687 the scan rate in the following order to 50, 25, 20, 15, 10, 5, 1 mV s^{-1} so as to
688 evaluate the dependency of peak current on the scan rate (data not shown). In
689 essence, it could be observed that the peak current was proportional to the
690 square root of scan rate, which implies diffusion limitations [65, 66]. Therefore,
691 it is to assume that the electron transfer from the biofilm to the anode could
692 have taken place via redox mediators [67], rather than through a direct
693 connection established between the cell membrane-bound redox enzymes and

694 the terminal electron acceptor (anode). According to the peak shifting
695 phenomenon the systems could be considered as quasi-reversible with 'slow'
696 electron transfer process taking place [64]. Since the redox peak areas
697 increased simultaneously with the current generated (as described in Section
698 3.1.), it would appear that these electron-shuttling substances were secreted
699 by the electroactive bacteria. From a stability point of view, the increasing or
700 constant value of the current peaks can be considered as an implicit indicator
701 of proper and developing exoelectrogenic activity [64].

702 In summary, based on the above discussion, it can be concluded that
703 anodes in both MFCs developed in a comparable way over time and the
704 involvement of (similar) endogenous redox mediators in accomplishing
705 mediated electron transfer can be supposed. Additionally, no limitation or
706 negative impact ascribed to the application of SILM appeared on the
707 electrochemical activity (relative to Nafion). However, further experiments will
708 be needed to study the membrane characteristics (e. g. swelling, stability,
709 resistance to biofouling, etc.) and their change over time, which are crucial
710 aspects of membrane development for bioelectrochemical applications [68], in
711 agreement with the implications made in the last paragraph of Section 3.1.

712

713 **3.7. Analysis of MFC internal resistance breakdown by electrochemical** 714 **impedance spectroscopy (EIS)**

715

716 The similar development of bioelectrochemical activity in the MFCs over
717 time was proved by the outcomes of biological and electrochemical process
718 characterization methods (Sections 3.5 and 3.6). EIS analysis is able to
719 provide more detailed insights to reveal how the total internal resistance of
720 MFC is influenced by the various factors. In fact, R_i can be considered as the
721 product of electrode (anode + cathode) charge transfer resistances (R_{CT}),
722 (solid + liquid) electrolyte (membrane + bulk solution) resistances (R_{M+S}) and
723 diffusion resistance (R_D), in accordance with Eq. 3.

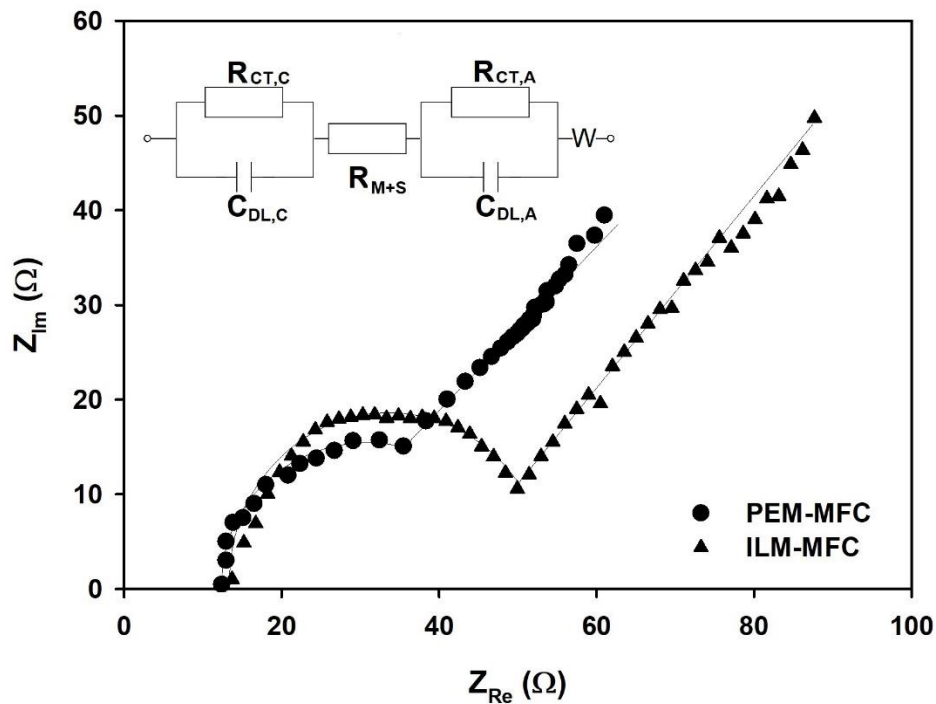
724

$$R_i = R_{CT} + R_{M+S} + R_D \quad (3)$$

726

727 Therefore, complete fuel cell EIS spectra were registered in the MFCs
 728 (**Fig. 8**) at the 21th day of operation (last cycle appearing in **Fig. 2**). As it is also
 729 shown in **Fig. 8**, a symmetric equivalent circuit model – containing anodic and
 730 cathodic charge transfer resistances (R_{CT}), combined membrane/solution
 731 resistances (R_{M+S}), capacitances of the electrical double layer (C_{DL}) and a
 732 Warburg element (W) – was used to represent the experimental system, as
 733 suggested by [Wei et al. \[69\]](#). By fitting this model to the data measured, R_{CT}
 734 and R_{M+S} could be obtained. As demonstrated by [Nam et al. \[70\]](#), once R_{CT}
 735 and R_{M+S} values are known, simple subtraction of those from R_i (according to
 736 Eq. 3) will lead to an estimate of the third resistance component, namely the
 737 diffusion resistance (R_D).

738



739

740 **Fig. 8** – The whole-cell EIS spectra (Nyquist plots) for PEM-MFC and ILM-
 741 MFC (including experimental and model data) and the equivalent circuit model
 742 of the bioelectrochemical cells.

743

744 The results of model fitting and the resistance values calculated are
 745 listed in **Table 5**. As it can be seen, only slight differences in terms of R_{M+S} and
 746 R_{CT} could be noted in the MFCs regardless of the membrane type. Hence, as
 747 the results implied, the major difference could be observed for the diffusion
 748 resistances: in case of PEM-MFCs 253.9 Ω , while in ILM-MFCs 213.2 Ω were
 749 obtained. This means that in both systems, R_D had the highest contribution to
 750 the actual R_i (84 and 79 %, respectively).

751

752 **Table 5 – Estimated values of different components of the total internal**
 753 **MFC resistance**

754

MFC type	R_{CT} (Ω)	R_{M+S} (Ω)	R_D (Ω)	R_i (Ω)
PEM-MFC	35.7 \pm 11.1	12.4 \pm 1.9	253.9 \pm 4	302 \pm 17
ILM-MFC	41.1 \pm 7.3	13.7 \pm 0.9	213.2 \pm 2.8	268 \pm 11

755

756 These findings are in agreement with literature data [69-71], where
 757 diffusion resistance was frequently reported as the dominant factor affecting
 758 the total internal resistance. Diffusion resistance is connected to the slow
 759 diffusion of various chemical species present in MFC systems. The lower R_D in
 760 case of ILM-MFC could suggest that the transport of species involved in the
 761 cathodic reduction reaction and/or affecting the cathodic (electrode)
 762 environment was less performance limiting using the SILM as physical
 763 separator. As a result, this assumed phenomenon, to a certain extent, could
 764 lead to the reduction of mass transport limitations in ILM-MFC. On the
 765 contrary, these transport processes might be more hindered/less
 766 advantageous (relative to ILM-MFC) applying PEM. This assumption could
 767 support the findings of polarization measurements (described in Section 3.4)
 768 and the conclusions regarding **Fig. 6**, according to which the differences in the
 769 membrane-related mass transport processes (indicated by steady-state
 770 discrete cathode potential values) seemed to be a reasonable explanation
 771 behind the better performance of ILM-MFC. Nevertheless, further experiments

772 targeting the in-depth evaluation of mass transfer processes are needed for a
773 better understanding of the main differences between the transfer mechanisms
774 taking place through the PEMs and SILMs.

775

776 **4. Conclusions**

777

778 In this work, the effect of membrane separators on the performance and
779 behavior of microbial fuel cells was addressed. Various techniques such as
780 cyclic voltammetry, dehydrogenase enzyme activity measurement, cell
781 polarization, electrochemical impedance spectroscopy, estimation of both
782 Coulombic efficiency and energy recovery were applied for a comparative
783 assessment. It has turned out that membranes prepared with [bmim][PF₆] ionic
784 liquid and PVDF support matrix, depending on the conditions, could be
785 employed more efficiently than Nafion, the most commonly applied proton
786 exchange membrane. The main reason for better performance of the former
787 system seemed to be in relation with the differences of mass transfer
788 phenomena taking place through the IL-based membrane separator. During
789 the experiments, the use of SILM had no observable negative effect on the
790 biological catalysts of the MFCs, while it could potentially lead to reduced
791 mass transport limitations and thus, higher MFC efficiency. Therefore,
792 membranes made with ionic liquids can have the potential to be used as
793 attractive separators in bioelectrochemical systems such as MFCs.

794 **Acknowledgements**

795

796 The János Bolyai Research Scholarship of the Hungarian Academy of
797 Sciences is duly acknowledged for the support. The “GINOP-2.3.2-15 –
798 Excellence of strategic R+D workshops (Development of modular, mobile
799 water treatment systems and waste water treatment technologies based on
800 University of Pannonia to enhance growing dynamic export of Hungary (2016-
801 2020))” is also thanked for supporting this work. Furthermore, this study was
802 financially supported by “Fondo de Sustentabilidad Energética SENER –
803 CONACYT (Mexico)”, through the project 247006 Gaseous Biofuels Cluster.
804 László Koók was supported by the ÚNKP-17-3 “New National Excellence
805 Program of the Ministry of Human Capacities”.

806

807 **References**

808

- 809 [1] B.E. Logan, B. Hamelers, R. Rozendal, U. Schröder, J. Keller, S.
810 Freguia, et al., Microbial fuel cells: Methodology and technology, Environ.
811 Sci. Technol. 40 (2006) 5181-5192.
- 812 [2] D. Pant, G. Van Bogaert, L. Diels, K. Vanbroekhoven, A review of the
813 substrates used in microbial fuel cells (MFCs) for sustainable energy
814 production, Bioresour. Technol. 101 (2010) 1533-1543.
- 815 [3] P. Pandey, V.N. Shinde, R.L. Deopurkar, S.P. Kale, S.A. Patil, D. Pant,
816 Recent advances in the use of different substrates in microbial fuel cells
817 toward wastewater treatment and simultaneous energy recovery, Appl.
818 Energy 168 (2016) 706-723.
- 819 [4] J.M. Sonawane, S.B. Adeloju, P.C. Ghosh, Landfill leachate: A promising
820 substrate for microbial fuel cells, Int. J. Hydrogen Energy 42 (2017)
821 23794-23798.
- 822 [5] G. Hernández-Flores, H.M. Poggi-Varaldo, T. Romero-Castañón, O.
823 Solorza-Feria, N. Rinderknecht-Seijas, Harvesting energy from leachates

- 824 in microbial fuel cells using an anion exchange membrane, *Int. J.*
825 *Hydrogen Energy* 42 (2017) 30374-30382.
- 826 [6] A. Colombo, A. Schievano, S.P. Trasatti, R. Morrone, N. D'Antona, P.
827 Cristiani, Signal trends of microbial fuel cells fed with different food-
828 industry residues, *Int. J. Hydrogen Energy* 42 (2017) 1841-1852.
- 829 [7] C. Lai, B. Li, M. Chen, G. Zeng, D. Huang, L. Qin, et al., Simultaneous
830 degradation of P-nitroaniline and electricity generation by using a
831 microfiltration membrane dual-chamber microbial fuel cell, *Int J Hydrogen*
832 *Energy* 43 (2018) 1749-1757.
- 833 [8] D. Cecconet, D. Molognoni, A. Callegari, A.G. Capodaglio, Agro-food
834 industry wastewater treatment with microbial fuel cells: Energetic
835 recovery issues, *Int. J. Hydrogen Energy* 43 (2018) 500-511.
- 836 [9] S.T. Oh, J.R. Kim, G.C. Premier, T.H. Lee, C. Kim, W.T. Sloan,
837 Sustainable wastewater treatment: How might microbial fuel cells
838 contribute, *Biotechnol. Adv.* 28 (2010) 871-881.
- 839 [10] H. Hiegemann, D. Herzer, E. Nettmann, M. Lübken, P. Schulte,
840 K.G. Schmelz, et al., An integrated 45 L pilot microbial fuel cell system
841 at a full-scale wastewater treatment plant, *Bioresour. Technol.* 218
842 (2016) 115-222.
- 843 [11] R. Liu, H. Tursun, X. Hou, F. Odey, Y. Li, X. Wang, et al.,
844 Microbial community dynamics in a pilot-scale MFC-AA/O system
845 treating domestic sewage, *Bioresour. Technol.* 241 (2017) 439-447.
- 846 [12] A. Escapa, M.I. San-Martín, R. Mateos, A. Morán, Scaling-up of
847 membraneless microbial electrolysis cells (MECs) for domestic
848 wastewater treatment: Bottlenecks and limitations, *Bioresour. Technol.*
849 180 (2015) 72-78.
- 850 [13] G. Kumar, P. Bakonyi, G. Zhen, P. Sivagurunathan, L. Koók, S.H.
851 Kim, et al., Microbial electrochemical systems for sustainable
852 biohydrogen production: Surveying the experiences from a start-up
853 viewpoint, *Renew. Sustain. Energy Rev.* 70 (2017) 589-597.

- 854 [14] C. Santoro, S. Rojas-Carbonell, R. Awais, R. Gokhale, M. Kodali,
855 A. Serov, et al., Influence of platinum group metal-free catalyst synthesis
856 on microbial fuel cell performance, *J. Power Sources* 375 (2018) 11-20.
- 857 [15] W.W. Li, G.P. Sheng, X.W. Liu, H.Q. Yu, Recent advances in the
858 separators for microbial fuel cells, *Bioresour. Technol.* 102 (2011) 244-
859 252.
- 860 [16] H. Zhang, S. Cheng, X. Wang, X. Huang, B.E. Logan, Separator
861 characteristics for increasing performance of microbial fuel cells, *Environ.*
862 *Sci. Technol.* 43 (2009) 8456-8461.
- 863 [17] M. Ollot, S. Galier, H. Roux de Balman, A. Bergel, Ion transport
864 in microbial fuel cells: Key roles, theory and critical review, *Appl. Energy*
865 183 (2016) 1682-1704.
- 866 [18] B.R. Dhar, H.S. Lee, Membranes for bioelectrochemical systems:
867 challenges and research advances, *Environ. Technol.* 34 (2013) 1751-
868 1764.
- 869 [19] T.H.J.A. Sleutels, A. ter Heijne, P. Kuntke, C.J.N. Buisman,
870 H.V.M. Hamelers, Membrane selectivity determines energetic losses for
871 ion transport in bioelectrochemical systems, *ChemistrySelect* 2 (2017)
872 3462-3470.
- 873 [20] M. Rahimnejad, G. Bakeri, M. Ghasemi, A. Zirepour, A review on
874 the role of proton exchange membrane on the performance of microbial
875 fuel cell, *Polym. Adv. Technol.* 25 (2014) 1426-1432.
- 876 [21] K.J. Chae, M. Choi, F.F. Ajayi, W. Park, I.S. Chang, I.S. Kim,
877 Mass transport through a proton exchange membrane (Nafion) in
878 microbial fuel cells, *Energy Fuels* 22 (2008)169-176.
- 879 [22] K.Y. Kim, K.J. Chae, M.J. Choi, E.T. Yang, M.H. Hwang, I.S. Kim,
880 High-quality effluent and electricity production from non-CEM based
881 flow-through type microbial fuel cell, *Chem. Eng. J.* 218 (2013) 19-23.
- 882 [23] S.E. Oh, B.E. Logan, Proton exchange membrane and electrode
883 surface areas as factors that affect power generation in microbial fuel
884 cells, *Appl. Microbiol. Biotechnol.* 70 (2006) 162-169.

- 885 [24] S. Angioni, L. Millia, G. Bruni, C. Tealdi, P. Mustarelli, E.
886 Quartarone, Improving the performances of Nafion™-based membranes
887 for microbial fuel cells with silica-based, organically-functionalized
888 mesostructured fillers, *J. Power Sources* 334 (2016) 120-127.
- 889 [25] J.R. Kim, S. Cheng, S.E. Oh, B.E. Logan, Power generation using
890 different cation, anion, and ultrafiltration membranes in microbial fuel
891 cells, *Environ. Sci. Technol.* 41 (2007) 1004-1009.
- 892 [26] V. Kumar, R. Rudra, A. Nandy, S. Hait, P.P. Kundu, Analysis of
893 partially sulfonated low density polyethylene (LDPE) membranes as
894 separators in microbial fuel cells, *RSC Adv.* 7 (2017) 21890-21900.
- 895 [27] X. Tang, K. Guo, H. Li, Z. Du, J. Tian, Microfiltration membrane
896 performance in two-chamber microbial fuel cells, *Biochem. Eng. J.* 52
897 (2010) 194-198.
- 898 [28] E. Yang, K.J. Chae, I.S. Kim, Assessment of different ceramic
899 filtration membranes as a separator in microbial fuel cells, *Desalin. Water*
900 *Treat.* 57 (2016) 28077-28085.
- 901 [29] J. Winfield, I. Gajda, J. Greenman, I. Ieropoulos, A review into the
902 use of ceramics in microbial fuel cells, *Bioresour. Technol.* 215 (2016)
903 296-303.
- 904 [30] D. Pant, G. Van Bogaert, Y. Alvarez-Gallego, L. Diels, K.
905 Vanbroekhoven, Evaluation of bioelectrogenic potential of four industrial
906 effluents as substrate for low cost Microbial Fuel Cells
907 operation, *Environ. Eng. Manag. J.* 51 (2016) 1897-1904.
- 908 [31] A.S. Mathuriya, D. Pant, Assessment of expanded polystyrene as
909 a separator in microbial fuel cell, *Environ. Technol.* (2018), doi:
910 <https://doi.org/10.1080/09593330.2018.1435740>
- 911 [32] F.J. Hernández-Fernández, A.P. de los Ríos, F. Mateo-Ramirez,
912 C. Godínez, L.J. Lozano-Blanco, J.I. Moreno, et al., New application of
913 supported ionic liquids membranes as proton exchange membranes in
914 microbial fuel cell for waste water treatment, *Chem. Eng. J.* 279 (2015)
915 115-119.

- 916 [33] L. Koók, N. Nemestóthy, P. Bakonyi, G. Zhen, G. Kumar, X. Lu, et
917 al., Performance evaluation of microbial electrochemical systems
918 operated with Nafion and supported ionic liquid membranes,
919 *Chemosphere* 175 (2017) 350-355.
- 920 [34] L. Koók, N. Nemestóthy, P. Bakonyi, A. Gölle, T. Rózsenszki,
921 P. Takács, et al., On the efficiency of dual-chamber biocatalytic
922 electrochemical cells applying membrane separators prepared with
923 imidazolium-type ionic liquids containing $[\text{NTf}_2]^-$ and $[\text{PF}_6]^-$ anions,
924 *Chem. Eng. J.* 324 (2017) 296-302.
- 925 [35] P. Bakonyi, L. Koók, E. Keller, K. Bélafi-Bakó, T. Rózsenszki,
926 G.D. Saratale, et al., Development of bioelectrochemical systems using
927 various biogas fermenter effluents as inocula and municipal waste liquor
928 as adapting substrate, *Bioresour. Technol.* 259 (2018)75-82.
- 929 [36] M. Ghasemi, W.R.W. Daud, M. Ismail, M. Rahimnejad, A.F.
930 Ismail, J.X. Leong, et al., Effect of pre-treatment and biofouling of proton
931 exchange membrane on microbial fuel cell performance, *Int. J.*
932 *Hydrogen Energy* 38 (2013) 5480-5484.
- 933 [37] L.E. Casida, D.A. Klein, T. Santoro, Soil dehydrogenase
934 activity, *Soil Science* 98 (1964) 371-376.
- 935 [38] M.V. Reddy, S. Srikanth, S.V. Mohan, P.N. Sarma, Phosphatase
936 and dehydrogenase activities in anodic chamber of single chamber
937 microbial fuel cell (MFC) at variable substrate loading conditions,
938 *Bioelectrochemistry* 77 (2010) 125-132.
- 939 [39] J. Wang, J. Luo, S. Feng, H. Li, Y. Wan, X. Zhang, Recent
940 development of ionic liquid membranes, *Green Energy Environ.* 1 (2016)
941 43-61.
- 942 [40] R. Fortunato, C.A.M. Afonso, J. Benavente, E. Rodriguez-
943 Castellón, J.G. Crespo, Stability of supported ionic liquid membranes as
944 studied by X-ray photoelectron spectroscopy, *J. Membr. Sci.* 256 (2005)
945 216-223.

- 946 [41] P. Wasserscheid, T. Welton, Ionic liquids in synthesis, John Wiley
947 & Sons, 2008.
- 948 [42] R. Fortunato, C.A.M. Afonso, M.A.M. Reis, J.G. Crespo,
949 Supported liquid membranes using ionic liquids: study of stability and
950 transport mechanisms, *J. Membr. Sci.* 242 (2004) 197-209.
- 951 [43] N. Nemestóthy, P. Bakonyi, T. Rózsenberszki, G. Kumar, L. Koók,
952 G. Kelemen, et al., Assessment via the modified gompertz-model reveals
953 new insights concerning the effects of ionic liquids on biohydrogen
954 production, *Int. J. Hydrogen Energy* 43 (2018) 18918-18924.
- 955 [44] M. Jebur, A. Sengupta, Y.H. Chiao, M. Kamaz, X. Qian, R.
956 Wickramasinghe, Pi electron cloud mediated separation of aromatics
957 using supported ionic liquid (SIL) membrane having antibacterial activity,
958 *J. Membr. Sci.* 556 (2018) 1-11.
- 959 [45] S. Roy, A. Schievano, D. Pant, Electro-stimulated microbial
960 factory for value added product synthesis, *Bioresour. Technol.* 213
961 (2016) 129-139.
- 962 [46] H. Liu, S. Cheng, B.E. Logan, Production of electricity from
963 acetate or butyrate using a single-chamber microbial fuel cell, *Environ.*
964 *Sci. Technol.* 39 (2005) 658-662.
- 965 [47] T.H.J.A. Sleutels, L. Darus, H.V.M. Hamelers, C.J.N. Buisman,
966 Effect of operational parameters on Coulombic efficiency in
967 bioelectrochemical systems, *Bioresour. Technol.* 102 (2011) 11172-
968 11176.
- 969 [48] S.V. Raghavulu, S.V. Mohan, R.K. Goud, P.N. Sarma. Effect of
970 anodic pH microenvironment on microbial fuel cell (MFC) performance in
971 concurrence with aerated and ferricyanide catholytes, *Electrochem.*
972 *Commun.* 11 (2009) 371-375.
- 973 [49] S.V. Mohan, R. Saravanan, S.V. Raghavulu, G. Mohanakrishna,
974 P.N. Sarma, Bioelectricity production from wastewater treatment in dual
975 chambered microbial fuel cell (MFC) using selectively enriched mixed
976 microflora: effect of catholyte, *Bioresour. Technol.* 99 (2008) 596-603.

- 977 [50] P. Bakonyi, L. Koók, G. Kumar, G. Tóth, T. Rózsenszki, D.D.
978 Nguyen, et al., Architectural engineering of bioelectrochemical systems
979 from the perspective of polymeric membrane separators: A
980 comprehensive update on recent progress and future prospects, *J.*
981 *Membr. Sci.* 564 (2018) 508-522.
- 982 [51] Z. Ge, J. Li, L. Xiao, Y. Tong, Z. He, Recovery of electrical energy
983 in microbial fuel cells, *Environ. Sci. Technol. Lett.* 1 (2014) 137-141.
- 984 [52] J. Li, H. Li, J. Zheng, L. Zhang, Q. Fu, X. Zhu, et al., Response of
985 anodic biofilm and the performance of microbial fuel cells to different
986 discharging current densities, *Bioresour. Technol.* 233 (2017) 1-6.
- 987 [53] S.V. Mohan, G. Mohanakrishna, S. Srikanth, P.N. Sarma,
988 Harnessing of bioelectricity in microbial fuel cell (MFC) employing
989 aerated cathode through anaerobic treatment of chemical wastewater
990 using selectively enriched hydrogen producing mixed consortia, *Fuel* 87
991 (2008) 2667-2676.
- 992 [54] F.J. Hernández-Fernández, A.P. de los Ríos, F. Mateo-Ramírez,
993 M.D. Juárez, L.J. Lozano-Blanco, C. Godínez, New application of
994 polymer inclusion membrane based on ionic liquids as proton exchange
995 membrane in microbial fuel cell, *Sep. Purif. Technol.* 160 (2016) 51-58.
- 996 [55] R.A. Rozendal, H.V.M. Hamelers, C.J.N. Buisman, Effects of
997 membrane cation transport on pH and microbial fuel cell performance,
998 *Environ. Sci. Technol.* 40 (2006) 5206-5211.
- 999 [56] F. Harnisch, U. Schröder, F. Scholz, The suitability of monopolar
1000 and bipolar ion exchange membranes as separators for biological fuel
1001 cells, *Environ. Sci. Technol.* 42 (2008) 1740-1746.
- 1002 [57] H. Rismani-Yazdia, S.M. Carver, A.D. Christy, O.H. Tuovinen,
1003 Cathodic limitations in microbial fuel cells: An overview, *J. Power*
1004 *Sources* 180 (2008) 683-694.
- 1005 [58] B.E. Logan, Exoelectrogenic bacteria that power microbial fuel
1006 cells, *Nature Rev. Microbiol.* 7 (2009) 375-381.

- 1007 [59] A.P. Borole, C.Y. Hamilton, T. Vishnivetskaya, D. Leak, C.
1008 Andras, Improving power production in acetate-fed microbial fuel cells via
1009 enrichment of exoelectrogenic organisms in flow-through systems,
1010 *Biochem. Eng. J.* 48 (2009) 71-80.
- 1011 [60] H.S. Park, B.H. Kim, H.S. Kim, H.J. Kim, G.T. Kim, M. Kim, et al.,
1012 A novel electrochemically active and Fe (III)-reducing bacterium
1013 phylogenetically related to *Clostridium butyricum* isolated from a
1014 microbial fuel cell, *Anaerobe* 7 (2001) 297-306.
- 1015 [61] K. Rabaey, N. Boon, S.D. Siciliano, M. Verhaege, W. Verstraete,
1016 Biofuel cells select for microbial consortia that self-mediate electron
1017 transfer, *Appl. Environ. Microbiol.* 70 (2004) 5373-5382.
- 1018 [62] S.V. Mohan, S.V. Raghavulu, P.N. Sarma, Influence of anodic
1019 biofilm growth on bioelectricity production in single chambered
1020 mediatorless microbial fuel cell using mixed anaerobic consortia, *Biosens.*
1021 *Bioelectron.* 24 (2008) 41-47.
- 1022 [63] S.A. Patil, F. Harnisch, B. Kapadnis, U. Schröder, Electroactive
1023 mixed culture biofilms in microbial bioelectrochemical systems: the role
1024 of temperature for biofilm formation and performance, *Biosens.*
1025 *Bioelectron.* 26 (2010) 803-808.
- 1026 [64] F. Harnisch, S. Freguia, A basic tutorial on cyclic voltammetry for
1027 the investigation of electroactive microbial biofilms, *Chem. Asian J.* 7
1028 (2012) 466-475.
- 1029 [65] A.J. Bard, L.R. Faulkner, *Electrochemical methods: Fundamentals*
1030 *and applications*, 2nd edition, John Wiley & Sons, Inc., 2001.
- 1031 [66] J. Babauta, R. Renslow, Z. Lewandowski, H. Beyenal,
1032 Electrochemically active biofilms: facts and fiction. A review, *Biofouling*
1033 28 (2012) 789-812.
- 1034 [67] S.B. Velasquez-Orta, I.M. Head, T.P. Curtis, K. Scott, Factors
1035 affecting current production in microbial fuel cells using different
1036 industrial wastewaters, *Bioresour. Technol.* 102 (2011) 5105-5112.

- 1037 [68] J.R. Varcoe, P. Atanassov, D.R. Dekel, A.M. Herring, M.A.
1038 Hickner, P.A. Kohl, et al., Anion-exchange membranes in
1039 electrochemical energy systems, *Energy Environ. Sci.* 7 (2014) 3135-
1040 3191.
- 1041 [69] B. Wei, J.C. Tokash, F. Zhang, Y. Kim, B.E. Logan,
1042 Electrochemical analysis of separators used in single-chamber, air-
1043 cathode microbial fuel cells, *Electrochim. Acta* 89 (2013) 45-51.
- 1044 [70] J.Y. Nam, H.W. Kim, K.H. Lim, H.S. Shin, B.E. Logan, Variation of
1045 power generation at different buffer types and conductivities in single
1046 chamber microbial fuel cells, *Biosens. Bioelectron.* 25 (2010) 1155-1159.
- 1047 [71] A.J. Hutchinson, J.C. Tokash, B.E. Logan, Analysis of carbon fiber
1048 brush loading in anodes on startup and performance of microbial fuel
1049 cells, *J. Power Sources* 196 (2011) 9213-9219.